ACS Macro Letters

Letter

pubs.acs.org/macroletters

Fluorescence Correlation Spectroscopy in Dilute Polymer Solutions: Effects of Molar Mass Dispersity and the Type of Fluorescent Labeling

David Schaeffel,[†] Stoyan Yordanov,[‡] Roland Hinrich Staff,[†] Andreas Kreyes,[†] Yi Zhao,[†] Manfred Schmidt,[§] Katharina Landfester,[†] Johan Hofkens,[‡] Hans-Jürgen Butt,[†] Daniel Crespy,[†] and Kaloian Koynov*[,†]

[†]Max Planck Institute for Polymer Research, Ackermannweg 10, 55128 Mainz, Germany

[‡]Department of Chemistry, KU Leuven, Celestijnenlaan 200F, 3001 Leuven, Belgium

[§]Institute for Physical Chemistry, University of Mainz, Jacob-Welder Weg 11, 55099 Mainz, Germany

Supporting Information

ABSTRACT: Fluorescence correlation spectroscopy (FCS) has become an important tool in polymer science. Among various other applications the method is often applied to measure the hydrodynamic radius and the degree of fluorescent labeling of polymers in dilute solutions. Here we show that such measurements can be strongly affected by the molar mass dispersity of the studied polymers and the way of labeling. As model systems we used polystyrene and poly(methyl methacrylate) synthesized by atom transfer radical polymerization or free-radical polymerization. Thus, the polymers were either end-labeled bearing one fluorophore per chain or side-labeled with a number of fluorophores per chain proportional to the degree of polymerization.The experimentally measured autocorrelation curves were fitted with a newly derived theoretical model that uses the Schulz−Zimm distribution function to describe the dispersity in the degree of polymerization. For end-labeled polymers having a molecular weight distribution close to Schulz−Zimm, the fits yield values of the number-average degree of polymerization and the polydispersity index similar to those obtained by reference gel permeation chromatography. However, for the side-labeled polymers such fitting becomes unstable, especially for highly polydisperse systems. Brownian dynamic simulations showed that the effect is due to a mutual dependence between the fit parameters, namely, the polydispersity index and the number-average molecular weight. As a consequence, an increase of the polydispersity index can be easily misinterpreted as an increase of the molecular weight when the FCS autocorrelation curves are fitted with a standard single component model, as commonly done in the community.

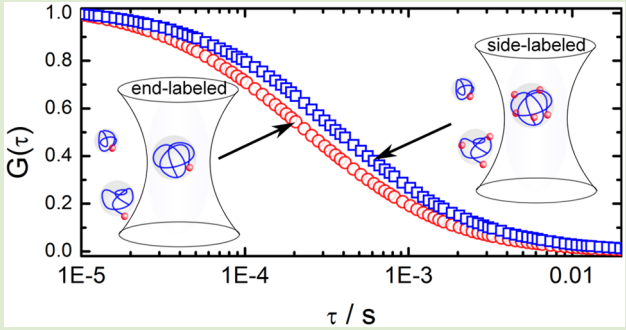

Fluorescence correlation spectroscopy (FCS) is a sensitive and selective technique for studying the mobility of fluorescent species, such as small molecules, macromolecules, or nanoparticles, in various environments.[1] Commonly, the diffusion coefficient, fluorescent brightness, and concentration of the fluorescent species are measured and used to assess their size, aggregation behavior, and interactions with other species or to obtain information about the surrounding environment.[1] While initially developed[2] and still predominantly used as a tool in molecular and cell biology[3,4] or to investigate colloidal systems,[5] during the past decade FCS has also become an established technique in polymer science.[6] For example, diffusion of molecular and macromolecular tracers in polymer solutions,[7−10] cross-linked polymer networks,[11−13] and bulk polymers[14] has been studied. FCS was also applied to investigate the interfacial diffusion of homo- and copolymers,[15,16] their self-assembly in micelles[17,18] or vesicles,[19,20] and even the process of polymerization itself.[21] One of the most characteristic properties of polymers is their molar mass dispersity. However, it is a common perception that compared to some classical techniques such as gel permeation chromatography (GPC) or photon correlation spectroscopy (PCS) FCS is not sensitive to moderate variations in the size of the studied polymers and thus to their molar mass dispersity. The reduced sensitivity is related to the rather slow, hyperbolic decay of the FCS autocorrelation function compared to the exponential decay in PCS. Thus, in many FCS studies of polymers the effect of polydispersity is neglected. Moreover, the method was never applied to explicitly measure the polydispersity index of flexible chain polymers in solutions. In this letter we show that in many practical cases polydispersity may strongly affect the experimentally measured FCS autocorrelation curves. If not properly accounted for, this leads to errors in the estimated average molecular weight. Here

Received: October 5, 2014
Accepted: January 7, 2015
Published: January 13, 2015

DOI: 10.1021/mz500638e
ACS Macro Lett. 2015, 4, 171−176

a key parameter is the kind of fluorescent labeling, e.g., end-chain labeling with one fluorophore per polymer chain vs side chain labeling, with a number of fluorophores proportional to the degree of polymerization. We explore these effects by deriving a new theoretical model for the FCS autocorrelation function in the case of polydisperse polymers and comparing it to experimentally measured data and Brownian dynamic simulations.

In a typical FCS experiment, a laser beam is tightly focused into a solution of the fluorescent species via a high numerical aperture microscope objective. The emitted fluorescence is collected by the same objective and, after passing through a dichroic mirror, an emission filter, and a confocal pinhole, delivered to a fast and sensitive detector, usually an avalanche photo diode. These arrangements lead to the formation of a subfemtoliter observation volume V_{obs} with a Gaussian ellipsoid shape. Only fluorescence emitted from species inside V_{obs} is detected. The Brownian diffusion of the fluorescent species in and out of the observation volume V_{obs} creates temporal fluctuations in the detected fluorescence intensity $\delta F(t)$ that are recorded and evaluated in terms of an autocorrelation function

$$G(\tau) = 1 + \frac{\langle \delta F(t)\delta F(t+\tau)\rangle}{\langle F(t)\rangle^2} \tag{1}$$

For an ensemble of identical, freely diffusing fluorescent species, not affected by photophysical processes such as transition to a triplet state, $G(\tau)$ has the following analytical form[1]

$$G(\tau;\, \tau_D) = 1 + \frac{1}{\langle N\rangle} M(\tau;\, \tau_D) \tag{2}$$

with

$$M(\tau;\, \tau_D) = \frac{1}{\left(1+\frac{\tau}{\tau_D}\right)\sqrt{1+\frac{\tau}{S^2\tau_D}}} \tag{3}$$

Here, $\langle N\rangle$ is the average number of fluorescent species in the observation volume; $S = z_0/r_0$ is the ratio of the axial to the radial dimension of V_{obs}; and τ_D is the species' diffusion time that is directly related to their diffusion coefficient

$$D = \frac{r_0^2}{4\tau_D} \tag{4}$$

and by the Stokes–Einstein relation to their hydrodynamic radius.

For a more complex system, in which the studied fluorescent species are not identical, the autocorrelation function can be expressed as

$$G(\tau) = 1 + \frac{1}{\langle N\rangle} \frac{\int_0^\infty P(\tau_D) M(\tau;\, \tau_D) \varepsilon(\tau_D)^2 \mathrm{d}\tau_D}{\left(\int_0^\infty P(\tau_D)\varepsilon(\tau_D)\mathrm{d}\tau_D\right)^2} \tag{5}$$

Here $P(\tau_D)$ is a size distribution function describing the number fraction of species with certain size and therefore certain diffusion coefficient and diffusion time τ_D. The fluorescent brightness distribution function $\varepsilon(\tau_D)$ accounts for the fact that the studied species may have also different fluorescent brightness, e.g., due to a different number of fluorophores attached to them.

Equation 5 was previously considered by Starchev et al.[22] who had approximated it by a sum of a large number (~30) of terms with discrete diffusion times using the method of histograms. While representing an experimental autocorrelation curve in this way is an ill-posed problem, by imposing additional regularization and constraint conditions the authors were able to estimate the polydispersity of dispersed colloidal particles. Following a similar approach, Sengupta et al.[23] have used a maximum entropy method based fitting routine (MEMFCS) to analyze FCS data for polydisperse systems in terms of a quasi-continuous distribution of diffusing components. Here we use a different approach, and instead of discretizing eq 5, we derive analytical expressions for $P(\tau_D)$ and $\varepsilon(\tau_D)$. In the case of fluorescently labeled synthetic polymers dissolved in a good solvent this can be done by correlating the diffusion time of an individual polymer chain to its degree of polymerization and then applying a common continuous distribution function to describe the dispersity in the degree of polymerization.

In dilute solutions the dynamics of a polymer chain with a high degree of polymerization is described by the Zimm model.[24] In the framework of this model, a scaling dependence of the chain diffusion coefficient D on the degree of polymerization X can be established. However, this relation is only an approximation and cannot be applied to flexible chains in good solvents due to the subtle influence of excluded volume effects. Thus, we used the empirical relation

$$D = KX^{-\nu} \tag{6}$$

which was shown to describe very well experimental data obtained by PCS.[25,26] K and ν are constants, which depend on the polymer and the solvent and can be obtained by fitting published data[25,26] on $D(X)$ with eq 6 as discussed below and in the Supporting Information (SI). Substituting eq 6 in eq 4 results in

$$\tau_D = \frac{r_0^2}{4K} X^\nu \tag{7}$$

Next, we consider the fluorescent brightness distribution function $\varepsilon(\tau_D)$ that is related to the number of fluorophores attached to a polymer chain with certain degree of polymerization X and thus certain diffusion time τ_D. Two common cases should be considered here:

(i) End chain labeling with one fluorophore per polymer chain and therefore $\varepsilon(X) = \text{const}$.
(ii) Side chain labeling, with a number of fluorophores proportional to the degree of polymerization and $\varepsilon(X) = F(X)$, where $F(X)$ is a proportionality function, depending on further specifics of the labeling procedure as discussed below.

With these considerations in mind and by inserting eq 7 in eq 3 to obtain an analytical expression for $M(\tau; X)$, eq 5 can be rewritten in the form

$$G(\tau) = 1 + \frac{1}{\langle N\rangle} \frac{\int_0^\infty P(X) M(\tau;\, X) \varepsilon(X)^2 \mathrm{d}X}{\left(\int_0^\infty P(X)\varepsilon(X)\mathrm{d}X\right)^2} \tag{8}$$

Here $P(X)$ is a continuous distribution function describing the dispersity in the degree of polymerization of the studied polymer system. For example, for polymers synthesized by atom transfer radical polymerization (ATRP) it was theoretically predicted that $P(X)$ should be a Poisson function. However, this prediction is based on the assumption of 100% monomer conversion and no side reactions[27] and thus is often

DOI: 10.1021/mz500638e
ACS Macro Lett. 2015, 4, 171−176

Table 1. Degree of Polymerization and Polydispersity Index of End-Labeled PMMA and PS Polymers as Evaluated by GPC and FCS[a]

	GPC		FCS: poly. fit (eq 8)			FCS: mono. fit (eq 2)	
sample	$\langle X\rangle$	PDI	$\langle X\rangle$	PDI	$\chi^2 \times 10^{-5}$	$X_{\mathrm{Mono.}}$	$\chi^2 \times 10^{-5}$
PMMA-I	149	1.33	111 ± 2	1.34 ± 0.07	1.5	102 ± 5	3.3
PMMA-II	188	1.17	145 ± 4	1.32 ± 0.1	3.2	133 ± 7	4.6
PS-I	76	1.21	62 ± 3	1.17 ± 0.13	11.6	60 ± 3	12.1
PS-II	87	1.24	81 ± 3	1.49 ± 0.12	3.8	72 ± 4	6.9

[a]The parameter (χ^2) represents the goodness of the fit.

not applicable to real systems. A more realistic distribution function describing the dispersity in the degree of polymerization is the Schulz−Zimm distribution[24]

$$P(X) = \frac{\xi^{\xi+1}}{\Gamma(\xi+1)}\frac{X^{\xi-1}}{\langle X\rangle^{\xi}}\exp\left(-\xi\frac{X}{\langle X\rangle}\right) \quad (9)$$

with $\langle X\rangle$ being the number-average degree of polymerization, Γ the gamma function, and $\xi = 1/(\mathrm{PDI} - 1)$ the chain coupling coefficient that is related to the polydispersity index PDI = M_w/M_n. Here M_w is the weight-average molecular weight and M_n the number-average molecular weight.

We used eq 8 to fit experimental autocorrelation curves measured for dilute toluene solutions of fluorescently labeled PS and PMMA and compared the obtained values of $\langle X\rangle$ and PDI with the results of GPC characterizations. A detailed description of the polymer synthesis and their characterization is given in the SI. The FCS experiments were performed on a commercial setup (Zeiss, Germany) consisting of the module ConfoCor2 and an inverted microscope model Axiovert 200, following a procedure reported earlier[14] and described in detail in the SI.

First, several polymers (Table 1) prepared by atom transfer radical polymerization (ATRP) were studied. The fluorophore was present in the initiator (SI), and thus one fluorophore was attached per polymer chain. Typical experimental autocorrelation curves and their corresponding fits using eq 8 are shown in Figure 1. The fitting was done using a standard least-squares nonlinear fitting procedure and numerically evaluating the integrals in eq 8 at each iteration step. Due to the one fluorophore per chain labeling the chain fluorescent brightness does not depend on the degree of polymerization, $\varepsilon(X)$ = const. This simplifies eq 8 and leaves only the average number of fluorescent species in the observation volume $\langle N\rangle$, the number-average degree of polymerization $\langle X\rangle$, and the polydispersity index PDI as fit parameters. For comparison the experimental data were also fitted with a single-component, "monodisperse" model (eq 2) as commonly done in previous studies. In this case the fit parameters were only $\langle N\rangle$ and X. For both types of fits the values of $K_{PS} = 1.598 \times 10^{-9}$ and $\xi_{PS} = 0.512$ for PS and $K_{PMMA} = 1.885 \times 10^{-9}$ and $\xi_{PMMA} = 0.526$ for PMMA were used to calculate the chain diffusion coefficient from its degree of polymerization. These values were obtained by fitting experimental data[25,26] on $D(X)$ with eq 6. Only data in the relatively narrow X range covering the values of X of the polymers listed in Table 1 were used (SI).

As can be seen in Figure 1a for a sample with moderate molar mass dispersity, PMMA-I ($\mathrm{PDI_{GPC}}$ = 1.33, Table 1), the polydisperse model provides distinctly better fit (lower and uniform residuals) than the monodisperse model. On the other hand as shown in Figure 1b, for polymers with lower molar mass dispersity, e.g., PS-I ($\mathrm{PDI_{GPC}}$ = 1.21, Table 1), the

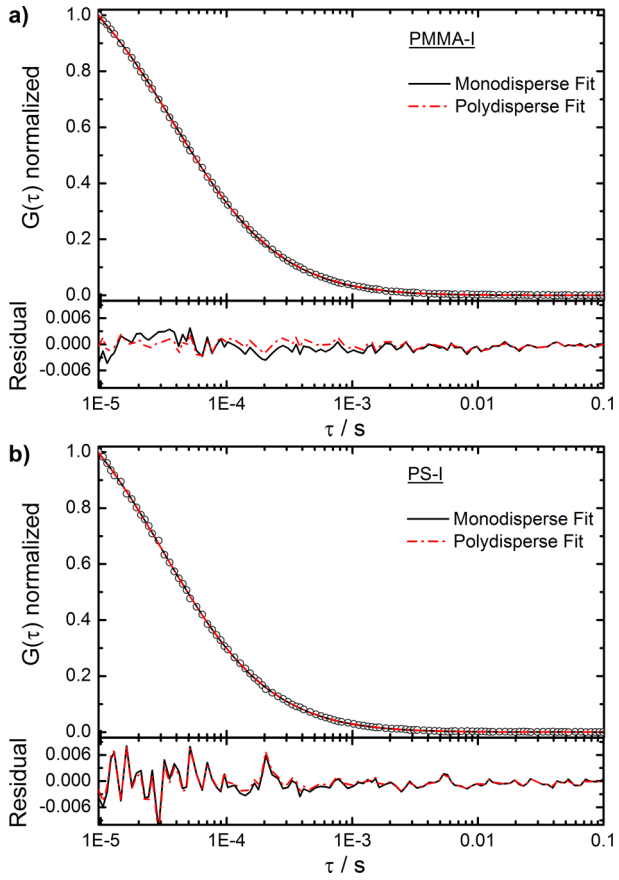

Figure 1. Experimental autocorrelation curves (symbols) measured in dilute (~10 nM) toluene solutions of the polymers PMMA-I (a) and PS-I (b). The lines in the upper panels represent the corresponding fits with the polydisperse (eq 8, dash dotted line) and the monodisperse (eq 2, straight line) models. The low panels show the corresponding residuals.

difference between the fits with the two models is barely visible. Nevertheless, even in this case the residuals (lower panel in Figure 1b) highlight a slight improvement in fitting when applying the polydisperse model. Moreover as shown in Table 1 for all studied polymers the polydisperse model yielded lower χ^2 values[28] and therefore better fits than the monodisperse model. These results indicate that FCS is sensitive even on small polydispersities of polymers. In the same time, our findings also demonstrate the existence of a lower border of PDI ≤ 1.2 below which no significant difference between the standard monodisperse model (eq 2) and the polydisperse model (eq 8) can be detected. The results from both types of fits for all studied samples are summarized in Table 1 and compared to the respective GPC data (SI). Fitting experimental FCS data of PS-I and PMMA-I with the polydisperse model

DOI: 10.1021/mz500638e
ACS Macro Lett. 2015, 4, 171−176

(Figure 1) yielded PDI values that within the error bars (nonlinear regression parameter confidence intervals of 95%) were identical to the corresponding GPC values. We emphasize here that the derived polydisperse FCS model (eq 8) relies on the similarity of the molar mass dispersity of the polymers to an ideal Schulz−Zimm distribution. PMMA-II and PS-II are examples where the size distribution deviated significantly from the Schulz−Zimm distribution (Figure S3c and d, SI). Correspondingly, the FCS yielded PDI values only in mediocre agreement with those from GPC. On the other hand, the good agreement between the GPC and FCS data for the sample PMMA-I shows that FCS can be used for measuring the molar mass dispersity of polymers even when the molar mass distribution moderately deviates from an ideal Schulz−Zimm distribution (Figure S3a, SI). With respect to the values of the average degree of polymerization $\langle X \rangle$ obtained with the polydisperse FCS model (Table 1) for PS the agreement with the corresponding GPC values is much better than for PMMA. This is probably caused by more accurate data for D vs X for PS than for PMMA (Figure S2, SI). At this point, it is also instructive to consider the results obtained by fitting the experimental FCS autocorrelation curves with the simple monodisperse model (eq 2) as is commonly done in most existing studies. The results summarized in Table 1 indicate that such a fit yields a degree of polymerization value that is relatively close to the number-average value obtained by the polydisperse FCS model fit or by GPC. Thus, the application of this simple FCS model to single fluorophore-labeled polymers is relatively safe and provides reasonable results.

The situation changes qualitatively for side chain labeling. Here the number of fluorophores per chain is proportional to the degree of polymerization. In such a case the dependence of the individual chain brightness on the degree of polymerization $\varepsilon(X) = F(X)$ has to be considered, which complicates eq 8 significantly. The physical picture is that the longer chains carry more fluorophores than the shorter ones and thus contribute stronger to the FCS autocorrelation curve, much as it happens in PCS. In order to study such a situation experimentally, we copolymerized styrene and methacrylate functionalized BODIPY dye in a free radical solution polymerization process yielding the polymer PS-III (SI). GPC revealed a number-average degree of polymerization $\langle X_{GPC} \rangle = 1863$ and a $PDI_{GPC} = 2.49$. Next, we recorded experimental FCS autocorrelation curves for dilute toluene solutions of PS-III and fitted them with eq 8. We used values of $K_{PS} = 2.304 \times 10^{-9}$ and $\nu_{PS} = 0.581$ to describe the relation between the diffusion coefficient and degree of polymerization (eq 6) for this high molecular weight sample (SI). Furthermore, the fits were done assuming linear dependence between the chain fluorescent brightness (number of fluorophores per chain) and the degree of polymerization, i.e., $\varepsilon(X) = AX$, with A = const. Such fitting, however, was not stable with respect to the starting values of the fitting parameters and thus failed to produce values of the degree of polymerization $\langle X_{FCS} \rangle$ and polydispersity index PDI_{FCS} consistent with the GPC results.

Thus, in order to prove the general validity of our approach and identify possible experimental pitfalls, we simulated "ideal experimental FCS autocorrelation curves" for a system with perfect Schulz−Zimm distribution and chain fluorescent brightness $\varepsilon(X) = AX$ and fitted them with eq 8. The simulation was done by adapting a previously proposed fast simulation algorithm[29] that produces autocorrelation curves for freely diffusing point-like particles with given diffusion coefficient and fluorescent brightness (SI). Briefly, the Schulz−Zimm distribution (eq 9) was used as a probability function for the generation of a chain with degree of polymerization X. To model the statistical labeling every 100th repeat unit was set as carrying a fluorophore, thus allowing only integer numbers of fluorophores per chain. This chain was then considered as a point-like particle with diffusion coefficient given by eq 6 and fluorescent brightness essentially linearly proportional to X. By generating a high number ($\sim 2 \times 10^5$) of such chains/particles and propagating them with Brownian dynamics procedure through the FCS probing volume,[29] a highly accurate autocorrelation curve was produced. Using this procedure we simulated experimental autocorrelation curves for PS with number-average degree of polymerization $\langle X_{Sim.} \rangle = 1000$ and different values of $PDI_{Sim.}$ ranging from 1.0 to 2.5. Typical curves and their fits with eq 8 assuming $\varepsilon(X) = AX$ are shown in Figure 2, and the

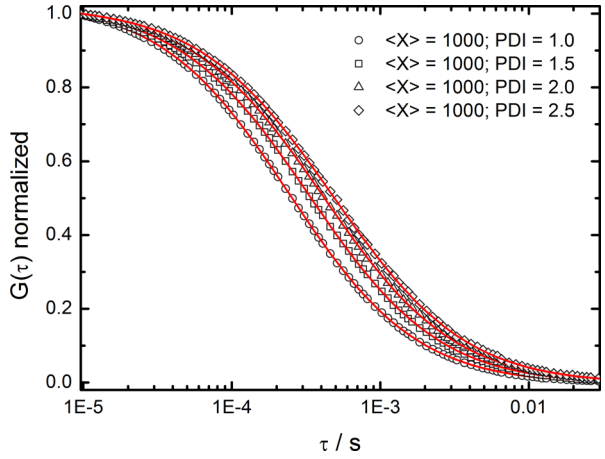

Figure 2. Simulated "experimental" FCS autocorrelation curves for statistically labeled polymers with different polydispersities (symbols) and their fits (lines) with eq 8. Also see Figure S5 (SI) for more details.

corresponding fit parameters are summarized in Table 2. The data show that in all cases the fitting yielded $\langle X \rangle$ and PDI values that within the fit errors are identical to the predefined values used in the simulations.

However, another important result from the fitting of the simulated autocorrelation curves (Table 2) is that when increasing the molar dispersity of the simulated polymer system, $PDI_{Sim.}$, from 1.0 to 2.5 the errors of the obtained fit parameters $\langle X_{FCS} \rangle$ and PDI_{FCS} (for a nonlinear regression

Table 2. Degree of Polymerization and the Polydispersity Index Obtained with FCS by Fitting Simulated Autocorrelation Curves for Statistically Labeled Polymers with Degree of Polymerization $\langle X_{Sim.} \rangle = 1000$ and $PDI_{Sim.}$ Ranging from 1.0 to 2.5

	polydisperse fit (eq 8)		monodisperse fit (eq 2)
$PDI_{Sim.}$	PDI_{FCS}	$\langle X_{FCS} \rangle$	$X_{Mono.}$
1.0	1.02 ± 0.02	979 ± 23	1031 ± 2
1.1	1.12 ± 0.04	983 ± 50	1201 ± 4
1.5	1.39 ± 0.15	1109 ± 162	1798 ± 13
2.0	1.79 ± 0.38	1150 ± 312	2607 ± 24
2.5	3.2 ± 2.22	762 ± 603	3458 ± 45

DOI: 10.1021/mz500638e
ACS Macro Lett. 2015, 4, 171−176

parameter confidence intervals of 95%) increase from roughly 2% to more than 80% (Table 2). This suggests an increasing mutual dependence between those two fit parameters. This mutual dependence is also evident when considering the autocorrelation curves shown in Figure 2. While all curves represent polymers with the same number-average degree of polymerization $\langle X \rangle$ = 1000, the increase of PDI has the same effect as an increase of $\langle X_{FCS} \rangle$, namely, shifts the decay of the correlation curves to higher lag times. The reason for this effect is the squaring of the fluorescent brightness $\varepsilon(X)$ in eq 8 which results in a stronger weighting of the longer, higher labeled polymer chains. This result clearly demonstrates the danger of using the simple monodisperse fit model (eq 2) with respect to such FCS data as it misinterprets the increase of PDI as an increase in the degree of polymerization (Table 2). Furthermore, our data suggest that for such ideally statistically labeled polymer systems a simple monodisperse fit will yield an X value that is even larger than the weight-average degree of polymerization. To confirm this effect on a real polymer system we performed a monodisperse fit (eq 2) to the experimentally measured FCS auto correlation curve for PS-III. As shown in Figure 3 such a fit seems to represent rather well the

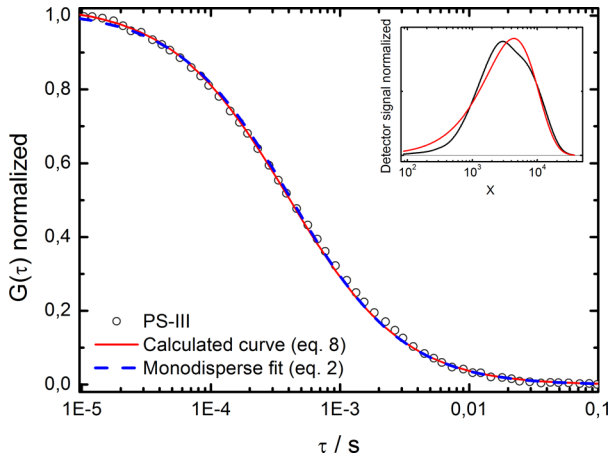

Figure 3. Experimental FCS autocorrelation curve measured in dilute toluene solutions of the polymer PS-III (symbols) and calculated FCS curve (solid line) using the polydisperse FCS model for a statistically labeled polymer (eq 8). The values of $\langle X \rangle$ and PDI in eq 8 were fixed to the corresponding GPC values. A fit with a simple monodisperse model (eq 2, dashed line) is also shown for comparison. The inset shows the GPC trace of PS-III (black line) and the fit with a Schulz–Zimm distribution (red line).

experimental data but overestimates significantly the degree of polymerization. It yields a value of X = 6670 that is significantly larger than the GPC result: X_n = 1863, X_w = 4638.

We now return to the polydisperse model FCS fit of the real polymer sample PS-III. It should be noted that the polydispersity of PS-III as measured by GPC is PDI_{GPC} = 2.49. A comparison with the simulated ideal samples (Table 2) shows that for $PDI_{Sim.}$ of 2.5 the FCS fit errors reach 80%. On the other hand, the real sample does not have an ideal Schulz–Zimm molar mass distribution (Figure 3), and the dependence between the number of fluorophores per chain and the degree of polymerization is not perfectly linear as confirmed by fractionation (see SI for details). Therefore, it is not surprising that the measured autocorrelation curve cannot be appropriately fitted with the model of eq 8. Thus, our results indicate that for highly polydisperse systems, with a PDI above 2.0, the model (eq 8) may not always provide a stable fit to experimental FCS data of statistically labeled polymers. Nevertheless, in order to further explore the limits of the model we applied it to fit the experimental data for sample PS-III, by fixing one of the parameters, either $\langle X \rangle$ or PDI, during the fitting procedure to its GPC value (SI). This yielded $\langle X_{FCS} \rangle$ = 1960 ± 47 and PDI_{FCS} = 2.60 ± 0.05, values that are basically identical to the GPC values showing the successful representation of the experimental data with eq 8. This is further illustrated in Figure 3 that compares the experimental autocorrelation curve of sample PS-III with a calculated curve using eq 8 with $\langle X \rangle$ or PDI fixed to their GPC values.

In conclusion, we have shown that when FCS is used to characterize fluorescently labeled polymers their polydispersity and type of fluorescent labeling play an important role. This can make the determination of the polymer hydrodynamic radius and thus estimation of the molecular weight nontrivial, particularly when experimental autocorrelation curves for polydisperse polymers are fitted with a simple monodisperse model as commonly carried out in existing studies. For polydisperse polymers bearing one (or a constant number) fluorophore per chain such fitting will provide the number-average value of the hydrodynamic radius. In contrast, if the number of fluorophores per chain is proportional to the degree of polymerization the fit will yield a significantly larger value. To address this issue we have derived a new model for the FCS autocorrelation function that uses the Schulz–Zimm distribution function to describe the dispersity in the degree of polymerization and an explicit relation to connect the chain diffusion coefficient to its molecular weight. The validity of the model and its limits were explored by comparing it to experimentally measured data and Brownian dynamic simulations.

■ ASSOCIATED CONTENT

Supporting Information

Synthesis of the MMA-BODIPY monomers, synthesis of BODIPY ATRP initiator, synthesis of PS and PMMA polymers, FCS, NMR, and GPC characterizations. This material is available free of charge via the Internet at http://pubs.acs.org.

■ AUTHOR INFORMATION

Corresponding Author

*E-mail: koynov@mpip-mainz.mpg.de.

Notes

The authors declare no competing financial interest.

■ ACKNOWLEDGMENTS

The financial support from DFG (SFB 1066, Q2) is gratefully acknowledged. R. H. Staff gratefully acknowledges financial support from the Fonds der Chemischen Industrie.

■ REFERENCES

(1) Rigler, R.; Elson, E. *Fluorescence correlation spectroscopy: theory and applications*; Springer series in chemical physics, 65; Springer: Berlin; New York, 2001.
(2) Magde, D.; Webb, W. W.; Elson, E. *Phys. Rev. Lett.* **1972**, *29*, 705.
(3) Hess, S. T.; Huang, S. H.; Heikal, A. A.; Webb, W. W. *Biochemistry* **2002**, *41*, 697–705.
(4) Kim, S. A.; Schwille, P. *Curr. Opin. Neurobiol.* **2003**, *13*, 583–590.
(5) Koynov, K.; Butt, H. J. *Curr. Opin. Colloid Interface Sci.* **2012**, *17*, 377–387.

DOI: 10.1021/mz500638e
ACS Macro Lett. 2015, 4, 171–176

(6) Woll, D. *RSC Adv.* **2014**, *4*, 2447−2465.
(7) Grabowski, C. A.; Mukhopadhyay, A. *Macromolecules* **2008**, *41*, 6191−6194.
(8) Cherdhirankorn, T.; Best, A.; Koynov, K.; Peneva, K.; Muellen, K.; Fytas, G. *J. Phys. Chem. B* **2009**, *113*, 3355−3359.
(9) Zettl, U.; Hoffmann, S. T.; Koberling, F.; Krausch, G.; Enderlein, J.; Harnau, L.; Ballauff, M. *Macromolecules* **2009**, *42*, 9537−9547.
(10) Szymanski, J.; Weiss, M. *Phys. Rev. Lett.* **2009**, *103*, 038102.
(11) Michelman-Ribeiro, A.; Boukari, H.; Nossal, R.; Horkay, F. *Macromolecules* **2004**, *37*, 10212−10214.
(12) Raccis, R.; Roskamp, R.; Hopp, I.; Menges, B.; Koynov, K.; Jonas, U.; Knoll, W.; Butt, H. J.; Fytas, G. *Soft Matter* **2011**, *7*, 7042−7053.
(13) Vagias, A.; Raccis, R.; Koynov, K.; Jonas, U.; Butt, H. J.; Fytas, G.; Kosovan, P.; Lenz, O.; Holm, C. *Phys. Rev. Lett.* **2013**, *111*, 088301.
(14) Cherdhirankorn, T.; Harmandaris, V.; Juhari, A.; Voudouris, P.; Fytas, G.; Kremer, K.; Koynov, K. *Macromolecules* **2009**, *42*, 4858−4866.
(15) Zhao, J.; Granick, S. *J. Am. Chem. Soc.* **2004**, *126*, 6242−6243.
(16) Yang, J. F.; Zhao, J.; Han, C. C. *Macromolecules* **2008**, *41*, 7284−7286.
(17) Bonne, T. B.; Ludtke, K.; Jordan, R.; Stepanek, P.; Papadakis, C. M. *Colloid Polym. Sci.* **2004**, *282*, 1425−1425.
(18) Bonne, T. B.; Ludtke, K.; Jordan, R.; Papadakis, C. M. *Macromol. Chem. Phys.* **2007**, *208*, 1402−1408.
(19) Mueller, W.; Koynov, K.; Fischer, K.; Hartmann, S.; Pierrat, S.; Basche, T.; Maskos, M. *Macromolecules* **2009**, *42*, 357−361.
(20) Jaskiewicz, K.; Larsen, A.; Schaeffel, D.; Koynov, K.; Lieberwirth, I.; Fytas, G.; Landfester, K.; Kroeger, A. *ACS Nano* **2012**, *6*, 7254−7262.
(21) Dorfschmid, M.; Mullen, K.; Zumbusch, A.; Woll, D. *Macromolecules* **2010**, *43*, 6174−6179.
(22) Starchev, K.; Buffle, J.; Perez, E. *J. Colloid Interface Sci.* **1999**, *213*, 479−487.
(23) Sengupta, P.; Garai, K.; Balaji, J.; Periasamy, N.; Maiti, S. *Biophys. J.* **2003**, *84*, 1977−1984.
(24) Rubinstein, M.; Colby, R. H. *Polymer Physics*; Oxford University Press: USA, 2003.
(25) Huber, K.; Bantle, S.; Lutz, P.; Burchard, W. *Macromolecules* **1985**, *18*, 1461−1467.
(26) Termeer, H. U.; Burchard, W.; Wunderlich, W. *Colloid Polym. Sci.* **1980**, *258*, 675−684.
(27) Lund, R.; Willner, L.; Pipich, V.; Grillo, I.; Lindner, P.; Colmenero, J.; Richter, D. *Macromolecules* **2011**, *44*, 6145−6154.
(28) Press, W. H.; Teukolsky, S. A.; Vetterling, W. T.; Flannery, B. P. *Numerical Recipes: The Art of Scientific Computing*, 3rd ed.; Cambridge University Press: New York, 2007.
(29) Schmitz, R.; Yordanov, S.; Butt, H.-J.; Koynov, K.; Dünweg, B. *Phys. Rev. E* **2011**, *84*, 066306.

DOI: 10.1021/mz500638e
ACS Macro Lett. 2015, 4, 171−176